

Dual oxygen and temperature sensing multi-task learning neural networks

FRANCESCA VENTURINI^{1,2,*}, UMBERTO MICHELUCCI², AND MICHAEL BAUMGARTNER¹

¹Institute of Applied Mathematics and Physics, Zurich University of Applied Sciences, Technikumstrasse 9, 8401 Winterthur, Switzerland

²TOELT LLC; Birchlenstr. 25, 8600 Dübendorf, Switzerland

*Corresponding author: francesca.venturini@zhaw.ch

Compiled January 7, 2020

A well-known optical approach to measure oxygen partial pressure is the quenching of luminescence by the oxygen molecules. Sensors based on this principle typically rely on approximate empirical models to parametrise the dependence of the sensing quantity on influencing factors, like the temperature. In this work, we propose a new multi-task learning (MTL) neural network approach which allows the extraction of both the oxygen concentration and the temperature using one single indicator and measuring a single quantity, namely the decay time. The results demonstrate that firstly, using neural networks it is possible to extract both the oxygen concentration and the temperature from the measurement of one single quantity and using one single indicator; secondly, that the use the proposed MTL networks allow more accurate and stable predictions for both the parameters. Furthermore, the proposed MTL approach is not limited to luminescence quenching but paves the way for applications where the mathematical model is not known, too complex or not really of interest.

© 2020 Optical Society of America under the terms of the [OSA Open Access Publishing Agreement](#)

<http://dx.doi.org/10.1364/optica.XX.XXXXXX>

1. INTRODUCTION

The determination of oxygen partial pressure is of great interest in numerous areas, like medicine, biotechnology, and chemistry. Among the different methods used to determine oxygen concentration, optical techniques are particularly attractive because they do not consume oxygen, have a fast response time, allow a good precision and accuracy. A well-known optical measuring approach is the quenching of luminescence by the oxygen molecules. The measuring principle is based on the measurement of the luminescence of a specific molecule, whose intensity and the decay time are reduced due to collisions with oxygen. Sensors based on this principle typically rely on approximate empirical models to parametrise the dependence of the sensing quantity on influencing factors. A new approach is to use feed-forward neural networks to predict the desired variables. Unfortunately, those kind of networks usually perform less efficiently when applied to multi-dimensional regression problems. In this work, we propose a new multi-task learning (MTL) neural network approach which allows the extraction of both the

oxygen concentration and the temperature using one single indicator and measuring a single quantity, namely the decay time. The results demonstrate that firstly, using neural networks it is in principle possible to extract both the oxygen concentration and the temperature from the measurement of one single quantity and using one single indicator; secondly, that the use the proposed MTL networks allow more accurate and stable predictions for both the parameters. Furthermore, the proposed MTL approach is not limited to luminescence quenching but may be of particular relevance in all those cases, where the mathematical model is not known, too complex or not really of interest and the only goal of the regression problem is to build a system that is able to determine as accurately as possible..

2. METHODS

A. Theoretical model for Luminescence Quenching for Oxygen Determination

B. Experimental Setup

The sample used for the characterization and test is a commercially available Pt-TFPP-based oxygen sensor spot (PSt3, PreSens Precision Sensing GmbH). To control the temperature of the samples, these were placed in good thermal contact with a copper plate, placed in a thermally insulated chamber. The temperature of this plate was adjusted at a fixed value between 5 °C and 45 °C in 5 °C steps using a Peltier element and stabilized with a temperature controller (PTC10, Stanford Research Systems). The thermally insulated chamber was connected to a self-made gas-mixing apparatus which enabled to vary the oxygen concentration between 0 % and 20 % vol O₂ by mixing nitrogen and dry air from two bottles. In the following, the concentration of oxygen will be given in % of the oxygen concentration of dry air and indicated with % air. This means, for example, that 20 % air corresponds to 4 % vol O₂ and 100 % air corresponds to 20 % vol O₂. The absolute error on the oxygen concentration adjusted with the gas mixing device is estimated to be below 1 % air. The oxygen concentration was varied between 0 % air and 100 % air in 5 % steps.

The optical setup used in this work for the luminescence measurements is shown schematically in Fig. 2.

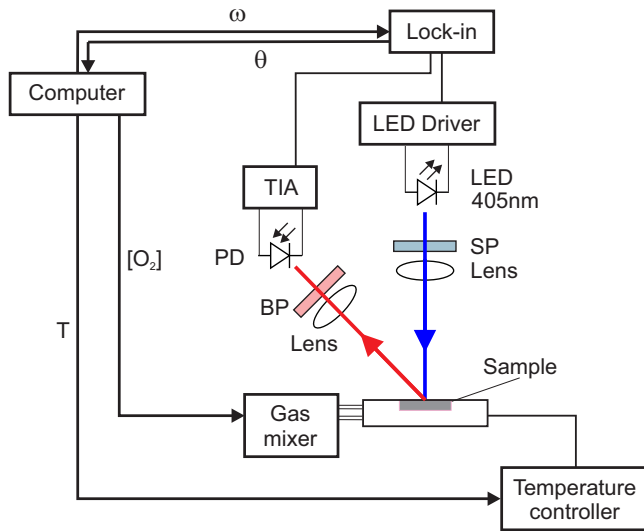


Fig. 1. Scheme of the optical experimental setup. Blue is the excitation, red the luminescence optical path. PD: photodiode; TIA: trans-impedance amplifier.

The excitation light was provided by a 405 nm LED (VAOL-5EUV0T4, VCC Visual Communications Company LLC), filtered by a short pass (SP) filter with cut-off at 498 nm (Semrock 498 SP Bright Line HC short pass) and focused on the surface of the samples with a collimation lens (EO43987, Edmund Optics). The luminescence was focussed by a lens (G063020000, LINOS) and collected by a photodiode (SFH 213 Osram). To suppress stray light and light reflected by the sample surface, the emission channel was equipped with a long pass filter with cut-off at 594 nm (Semrock 594 LP Edge Basic long pass) and a short pass filter with cut-off at 682 nm (Semrock 682 SP Bright Line HC short pass). The driver for the LED and the trans-impedance amplifier (TIA) are self-made. For the frequency generation

and the phase detection a two-phase lock-in amplifier (SR830, Stanford Research Inc.) was used. The modulation frequency was varied between 200 Hz and 15000 kHz.

C. Automated Data Acquisition

The series of measurements were carried out following the flow shown in Fig. XXX. First the acquisition program fixed the temperature and concentration. Then the phase-shift was measured for varying the modulation frequency. This measurement was repeated 20 times. Next, keeping the temperature fixed, the program changed the oxygen concentration and the entire frequency-loop was repeated. Finally, the temperature is changed and then the oxygen and frequency loops were repeated. The total number of measurements is $50 \times 20 \times 21 \times 9 = 189000$ which lasted ca. 65 hours. The number of measurement was chosen as a compromise between maximal number of measurements and minimal change of the sample due to photobleaching.

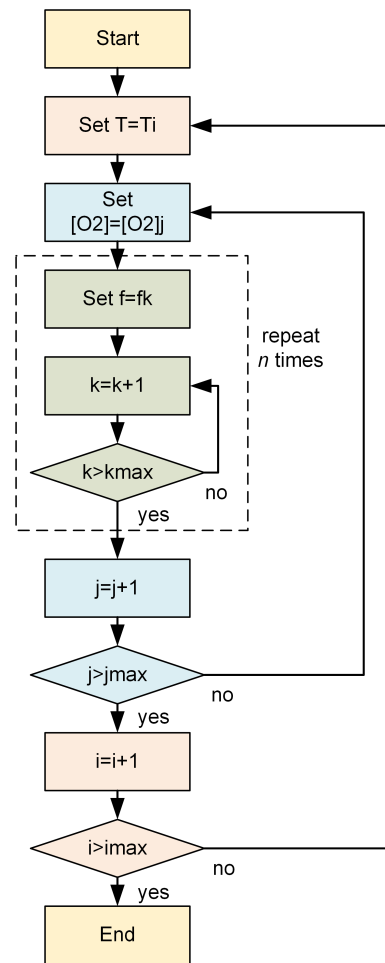


Fig. 2. Scheme of the optical experimental setup. Blue is the excitation, red the luminescence optical path. PD: photodiode; TIA: trans-impedance amplifier.

D. Artificial Neural Network Design

The MTL network proposed is depicted in Figure 3. It consists of three common hidden layers with 50 neurons each which generate as output a "shared representation". The name comes from the fact that the output of those layers is used to evaluate

both $[O_2]$ and T . These are followed by three branches, two with each two additional "task-specific hidden layers" to predict respectively $[O_2]$ and T , and then one without additional layers to predict $[O_2]$ and T at the same time. The shared representation is the input of two "task-specific hidden layers", that learn how to predict $[O_2]$ and T better. Note how the common hidden layers are shared with both the tasks of predicting $[O_2]$ and T , while the task-specific hidden layers are specific to each task separately. Therefore, the MTL network uses the common hidden layers to find common features beneficial to each of the two tasks. During the training phase, learning to predict $[O_2]$ will influence the common hidden layers and therefore, the prediction of T , and vice-versa. A set of task-specific hidden layers will then learn specific features to each output and therefore improve the prediction accuracy. The number of neurons of each task-specific hidden layer is 5.

In the three architectures investigated the sigmoid activation functions was used for all the neurons.

A common choice for the cost function in regression problems is the mean square error (MSE), which is defined as

$$MSE = \frac{1}{n} \sum_{j=1}^n \sum_{k=1}^d (y_k^{[j]} - \hat{y}_k^{[j]})^2 \quad (1)$$

where n is the number of observations in the input dataset; $y^{[j]} \in \mathbb{R}^d$ is the measured value of the desired quantity for the j^{th} observation (indicated as a superscript between square brackets), with $j = 1, \dots, n$; $\hat{y}^{[j]} \in \mathbb{R}^d$ is the output of the network, when evaluated on the j^{th} observation. Since there are multiple branches, a global cost function L needs to be defined as a linear combination of the task-specific cost functions with weights α_i will be minimized

$$L = \sum_{i=1}^{n_T} \alpha_i L_i. \quad (2)$$

The parameters α_i have to be determined during the hyper-parameter tuning phase to optimize the network predictions. In this paper, being the cost function the MSE (Equation 1), the global cost function of Equation 2 is

$$L = \sum_{i=1}^{n_T} \alpha_i \frac{1}{n} \sum_{j=1}^n \sum_{k=1}^d (y_k^{[j]} - \hat{y}_k^{[j]})^2 \quad (3)$$

where n_T is the number of tasks; n is the number of observations in the input dataset; $y^{[j]} \in \mathbb{R}^d$ is the measured value of the desired quantity for observation j , with $j = 1, \dots, n$; $\hat{y}^{[j]} \in \mathbb{R}^d$ is the output of the network, when evaluated on the j^{th} observation. The global cost function weights used for the plots were $\alpha_1 = 0.3$, $\alpha_2 = 5$ and $\alpha_3 = 1$. Those values were chosen because they result in the lowest MAEs (see discussion in Section ??).

To minimize the cost function, the optimizer Adaptive Moment Estimation (Adam) [1, 2] was used. The training was performed with a starting learning rate of 10^{-3} and using batch-learning, which means that the weights were updated only after the entire training dataset has been fed to the network. Batch-learning was chosen because of its stability and speed since it reduces the training time of a few orders of magnitude in comparison to, for example, stochastic gradient descent [1]. Therefore it makes experimenting with different networks a feasible endeavor. The implementation was performed using the TensorFlow library.

The metric used to compare results from different network models is the absolute error (AE) defined as the absolute value

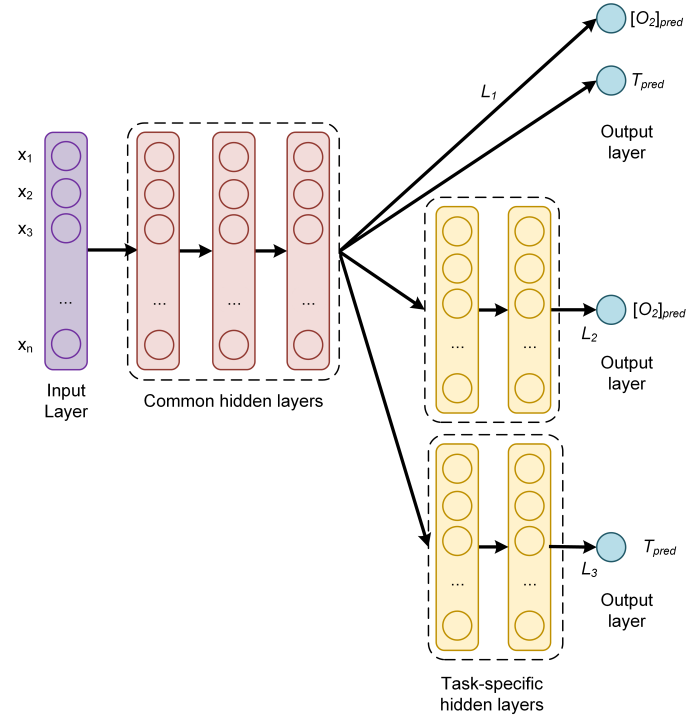


Fig. 3. Architecture of the feed-forward MTL.

of the difference between the predicted and the expected value for a given observation. For the oxygen concentration of the j^{th} observation $[O_2]^{[j]}$ the AE is

$$AE_{[O_2]}^{[j]} = |[O_2]_{pred}^{[j]} - [O_2]_{meas}^{[j]}|. \quad (4)$$

The further quantity used to analyze the performance of the network is the mean absolute error (MAE), defined as the average of the absolute value of the difference between the predicted and the expected oxygen concentration or temperature. For example, for the oxygen prediction using the training dataset S_{train} , $MAE_{[O_2]}$ is defined as

$$MAE_{[O_2]}(S_{train}) = \frac{1}{|S_{train}|} \sum_{j \in S_{train}} |[O_2]_{pred}^{[j]} - [O_2]_{real}^{[j]}| \quad (5)$$

where $|S_{train}|$ is the size (or cardinality) of the training dataset. For example, in this work $|S_{train}|=20000$. The AE_T and MAE_T are similarly defined.

3. RESULTS AND DISCUSSION

??

A. Sample Table

Table 1 shows an example table.

4. CONCLUSIONS

DISCLOSURES

Disclosures. The authors declare no conflicts of interest.

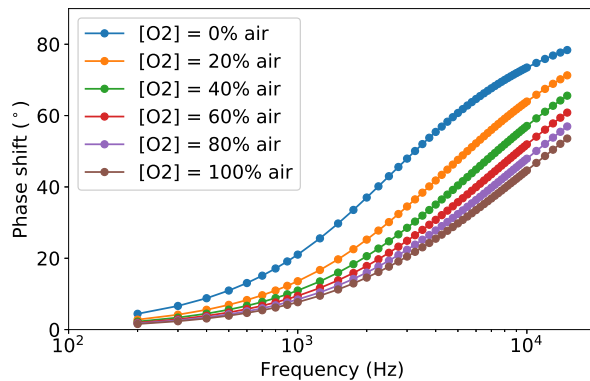


Fig. 4. At temperature 25....

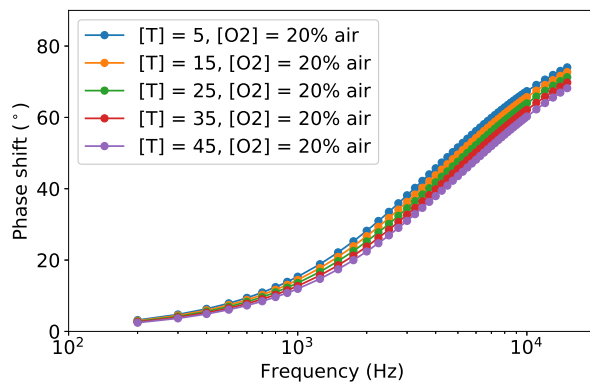


Fig. 5.

Table 1. Shape Functions for Quadratic Line Elements

| local node | $\{N\}_m$ | $\{\Phi_i\}_m$ ($i = x, y, z$) |
|------------|-----------------|----------------------------------|
| $m = 1$ | $L_1(2L_1 - 1)$ | Φ_{i1} |
| $m = 2$ | $L_2(2L_2 - 1)$ | Φ_{i2} |
| $m = 3$ | $L_3 = 4L_1L_2$ | Φ_{i3} |

SUPPLEMENTAL DOCUMENTS

Optica authors may include supplemental documents with the primary manuscript. For details, see [Supplementary Materials in Optica](#). To reference the supplementary document, the statement “See Supplement 1 for supporting content.” should appear at the bottom of the manuscript (above the references).

REFERENCES

For references, you may add citations manually or use BibTeX. E.g. [1].

Letter submissions to *Optica* require two sets of references: an abbreviated reference style for publication and a full reference list to aid the editor and reviewers. Citations to journal articles in the abbreviated list should omit the article title and final page number; this abbreviated reference style is produced automatically when the `\setboolean{shortarticle}{true}` option is selected in the template, if you are using a .bib file for your references.

The full reference list meant to aid the editor and reviewers must be included as well on an informational page that will not count against page length; again this will be produced automatically if you are using a .bib file and have the `\setboolean{shortarticle}{true}` option selected.

REFERENCES

1. Y. Zhang, S. Qiao, L. Sun, Q. W. Shi, W. Huang, L. Li, and Z. Yang, “Photoinduced active terahertz metamaterials with nanostructured vanadium dioxide film deposited by sol-gel method,” *Opt. Express* **22**, 11070–11078 (2014).

REFERENCES

1. Michelucci, U. *Applied Deep Learning - A Case-Based Approach to Understanding Deep Neural Networks*; Apress Media, LLC: New York, NY, USA, 2018; pp. 374–375.
2. Kingma, D.P.; Ba, J. Adam: A method for stochastic optimization. In Proceedings of 3rd International Conference on Learning Representations, ICLR 2015, San Diego, CA, USA, May 7-9, 2015, pp. 1–15.
3. Michelucci, U.; Baumgartner, M.; Venturini, F. Optical oxygen sensing with artificial intelligence. *Sensors* **2019**, *19*, 777.
4. Michelucci, U.; Venturini, F. Multi-Task Learning for Multi-Dimensional Regression: Application to Luminescence Sensing. *Appl. Sci.* **2019**, *9*, 4748.